J. Phycol. **38,** 1132–1142 (2002)

DIEL VARIATIONS IN OPTICAL PROPERTIES OF *MICROMONAS PUSILLA* (PRASINOPHYCEAE)[1]

Michele D. DuRand,[2] *Rebecca E. Green, Heidi M. Sosik,*[3] *and Robert J. Olson*

Woods Hole Oceanographic Institution, Biology Department, MS #32, Woods Hole, Massachusetts 02543, USA

***Micromonas pusilla* (Butcher) Manton et Parke, a marine prasinophyte, was used to investigate how cell growth and division affect optical properties of phytoplankton over the light:dark cycle. Measurements were made of cell size and concentration, attenuation and absorption coefficients, flow cytometric forward and side light scattering and chl fluorescence, and chl and carbon content. The refractive index was derived from observations and Mie scattering theory. Diel variations occurred, with cells increasing in size, light scattering, and carbon content during daytime photosynthesis and decreasing during nighttime division. Cells averaged 1.6 μm in diameter and exhibited phased division, with 1.3 divisions per day. Scattering changes resulted primarily from changes in cell size and not refractive index; absorption changes were consistent with a negligible package effect. Measurements over the diel cycle suggest that in *M. pusilla* carbon-specific attenuation varies with cell size, and this relationship appears to extend to other phytoplankton species. Because *M. pusilla* is one of the smallest eukaryotic phytoplankton and belongs to a common marine genus, these results will be useful for interpreting *in situ* light scattering variation. The relationship between forward light scattering (FLS) and volume over the diel cycle for *M. pusilla* was similar to that determined for a variety of phytoplankton species over a large size range. We propose a method to estimate cellular carbon content directly from FLS, which will improve our estimates of the contribution of different phytoplankton groups to productivity and total carbon content in the oceans.**

Key index words: **absorption; attenuation; diel variation; flow cytometry; *Micromonas pusilla*; optical properties; phytoplankton; *Prasinophyceae*; refractive index; scattering**

Abbreviations: ***a*, absorption coefficient; a^*_{chl}, chl-specific absorption coefficient; ac-9, absorption and attenuation meter; *b*, scattering coefficient; b^*_{chl}, chl-specific scattering coefficient; *c*, attenuation coefficient; c_c^*, carbon-specific attenuation coefficient; C_i, intracellular carbon concentration; C:N, carbon to nitrogen ratio; Chl_i, intracellular chlorophyll concentration; CV, coefficient of variation; $\overline{D}$, the diameter of the mean cell; FLS, forward light scattering; $\overline{G}$, geometric projected area of the mean cell; γ, spectral slope; μ, growth rate; n, real refractive index; n', imaginary refractive index; σ_a, absorption cross-section; σ_b, scattering cross-section; σ_c, attenuation cross-section; Q_a, efficiency factor for absorption; Q_b, efficiency factor for scattering; Q_c, efficiency factor for attenuation; $\overline{V}$, volume of the mean cell**

INTRODUCTION

Diel variations in bulk optical properties such as beam attenuation (Siegel et al. 1989, Hamilton et al. 1990, Cullen et al. 1992, Stramska and Dickey 1992, Gardner et al. 1993, 1995) and in single cell optical properties such as phytoplankton forward light scattering (FLS) (Olson et al. 1990, DuRand and Olson 1996, Vaulot and Marie 1999) have been observed in numerous field studies in many of the world's oceans. A number of researchers have documented diel variations in cell light scattering during laboratory studies of various phytoplankton cultures (Stramski and Reynolds 1993, Stramski et al. 1995, DuRand and Olson 1998). The typical pattern exhibited is scattering minima at dawn and maxima near dusk. Diel variations in beam attenuation have been related to primary production (Siegel et al. 1989, Cullen et al. 1992, Walsh et al. 1995) and have been proportioned among groups of organisms in the ocean (DuRand 1995, DuRand and Olson 1996, Chung et al. 1998, Binder and DuRand 2002).

Light scattering by particles such as phytoplankton is determined by their size and refractive index and, to a lesser extent, by their shape and internal structures (Jerlov 1976). If diel changes in scattering cross-sections can be related to changes in cell size and carbon content, then phytoplankton productivity (Cullen et al. 1992) and growth rates (DuRand 1995, Binder et al. 1996) can be estimated from measurements over the diel cycle in the field. In laboratory studies, contrasting data have been obtained on the relative contributions of variations in particle size and in refractive index to diel changes in optical cross-sections. Changes in refractive index have been found to be equal to or more important than changes in cell size for determining the attenuation cross-section of a diatom (Stramski and Reynolds 1993) and a prokary-

[1]Received 24 January 2002. Accepted 22 June 2002.

[2]Present address: Ocean Sciences Centre, Memorial University of Newfoundland, St. John's, NL A1C 5S7, Canada. E-mail mdurand@mun.ca.

[3]Author for correspondence: e-mail hsosik@whoi.edu.

otic picoplankter (Stramski et al. 1995). In contrast, DuRand and Olson (1998) reported that changes in cell size were more important than those in refractive index in determining diel variations in beam attenuation for a small chlorophyte.

Estimates of primary production in the ocean have been made from diel variations in beam attenuation by converting changes in beam attenuation to carbon production using a constant factor (Siegel et al. 1989, Cullen et al. 1992, Walsh et al. 1995). Ackleson et al. (1993), however, reported carbon-independent changes in cell scattering. In addition, several other laboratory studies on cultures have found that the carbon-specific beam attenuation varies by 25%–30% over the diel cycle (usually increasing during the day) and mean values among the species studied vary by ±21% (Stramski and Reynolds 1993, Stramski et al. 1995, DuRand and Olson 1998). It may be necessary to know the composition of the phytoplankton community to best interpret diel variations in beam attenuation as production (DuRand and Olson 1996, Binder and DuRand 2002).

Stramski (1999) suggested that the strong correlation between intracellular carbon concentration and real refractive index and between intracellular chl concentration and the imaginary refractive index, observed for phytoplankton cultures, could be used to estimate carbon and chl content of individual cells in natural water samples. Despite the fact that the derivation of refractive index from single-particle analysis is not currently routine, the results of such an approach are appealing because knowledge of the carbon-based size distribution of the plankton is crucial to an understanding of upper ocean carbon cycling and knowledge of chl per cell is important for studies of phytoplankton productivity and for bio-optical modeling.

Flow cytometric analyses of natural samples have shown that eukaryotic picophytoplankton are ubiquitous (e.g. DuRand and Olson 1996, Campbell et al. 1997, Zubkov et al. 1998, Shalapyonok et al. 2001), but detailed laboratory studies of diel variations in phytoplankton optical properties have focused on smaller and larger cell types, including prokaryotic picoplankton (Stramski et al. 1995) and eukaryotic nanoplankton (e.g. Stramski and Reynolds 1993, DuRand and Olson 1998). To fill this gap, we chose to examine a small (approximately 1.6 μm diameter) prasinophyte, *Micromonas pusilla*; recent studies on picoplankton diversity using molecular approaches suggest that prasinophytes, and the genus *Micromonas* in particular, are important in many different environments from open ocean to coastal waters (Diez et al. 2001, Not et al. 2002, F. Not and D. Vaulot, personal communication). Here we examine variations in physical, chemical, and optical properties over the diel cycle. In addition, we evaluate the relative importance of cell size and refractive index to changes in optical properties, examine variability in the carbon-specific beam attenuation, and propose a method to estimate cellular carbon for different phytoplankton groups directly from flow cytometric FLS and an empirical calibration.

MATERIALS AND METHODS

Laboratory measurements. Micromonas pusilla (CCMP 489), a strain isolated from the Sargasso Sea, was grown in f/2 medium without silica (Guillard 1975) in replicate batch cultures at 25° C. The filtered (0.22 μm) seawater and nutrient solutions were autoclaved separately and then added together after the seawater had cooled. To ensure particle-free medium, the solution was then sterile filtered through a 0.22-μm filter. The cultures were grown in 10-L carboys (containing 2 L of culture at the start of sampling) in an incubator on a 12:12-h light:dark cycle at 120 μmol photons·m^{-2}·s^{-1} (cool-white fluorescent lights, measured with a QSL-100 4π quantum scalar irradiance sensor, Biospherical Instruments, San Diego, CA, USA). The carboys were bubbled with moisturized filtered air. Samples were forced out by air pressure through a sterile sampling port. The cultures were acclimated to the growth conditions for 7 days and diluted daily for 5 days before the day of sampling (with the last dilution 24 h before the start of the sampling) to maintain the cells in exponential growth.

Samples were withdrawn every 2 h (starting at dawn, until the following dawn) and measurements made of cellular and bulk properties (individual cell measurements of concentration, forward and side light scattering, chl fluorescence, and cell size, and bulk measurements of absorption, attenuation, extracted chl content, and carbon content). Samples were processed in dim light during the nighttime sampling points.

A modified Epics V flow cytometer (Beckman Coulter, Miami, FL, USA) with a C*i*cero acquisition interface (Cytomation, Fort Collins, CO, USA) was used to measure FLS (3–19° at 488 nm), side angle light scattering (~54–126° at 488 nm), and chl fluorescence (660–700 nm) of the *M. pusilla* cells in undiluted duplicate samples. Polystyrene microspheres of two sizes (0.66 μm and 2.14 μm, YG calibration-grade beads from Polysciences, Warrington, PA, USA) were added as internal standards and differentiated from cells by their orange fluorescence (555–595 nm). The samples were introduced into the flow cytometer using a peristaltic pump (Harvard Apparatus, Holliston, MA, USA), and cell concentration was determined from the pump flow rate and sample run time. Mean values of the measured parameters normalized to reference beads (2.14 μm) were calculated using "CYTOWIN" software (D. Vaulot, www.sb-roscoff.fr/Phyto/cyto.html).

The size distribution of the *M. pusilla* cells was determined using a Coulter Multisizer (Beckman Coulter, Miami, FL, USA) equipped with a 30-μm aperture. The culture was diluted with filtered seawater (9- to 14-fold dilutions) to obtain coincidence rates of 6% or less. The size distributions of replicate samples were averaged and normalized to the cell concentration from flow cytometric analysis. These average 256-channel data of cell diameter distributions were used to calculate the geometric projected area of the mean cell ($\overline{G}$, μm^2), the diameter of the mean cell ($\overline{D}$, μm), and the volume of the mean cell ($\overline{V}$, μm^3) to include the effects of polydispersion in subsequent calculations (equations from Stramski and Reynolds 1993, Reynolds et al. 1997).

Spectral absorption and attenuation at nine wavelengths (412, 440, 488, 510, 532, 555, 650, 676, and 715 nm) were measured using an absorption and attenuation meter with a 25-cm pathlength (ac-9, WETLabs, Philomath, OR, USA). Two reservoirs were attached with tubing to the inlet and outlet of the ac-9, samples (diluted 9- to 21-fold with filtered seawater) were gravity fed through the instrument, and data collection was closely monitored to ensure the absence of air bubbles. A dilution series was measured at the start of the experiment to ensure that operation was within the linear range of the instrument. Filtered seawater was run between consecutive samples and subtracted as a blank. A temperature correction was applied to account for the difference between water temperature of the samples and that during instrument calibration (Pegau et al. 1997). The measured absorption and attenuation coefficients (a and c, m^{-1}) were normalized to the cell concentrations to obtain average cross-sections (σ_a and σ_c, μm^2). The measured efficiency factors for attenuation (Q_c) were determined as $\sigma_c/\overline{G}$.

Absorption was measured in a 1-cm cuvette using a Lambda 18 UV/VIS dual-beam spectrophotometer with a 60-mm integrating sphere (Perkin-Elmer, Shelton, CT, USA). Syringe-filtered (0.22 μm) culture was used in the reference cuvette and as the blank. A dilution series was measured at the start of the experiment to ensure that in subsequent measurements multiple scattering effects were negligible. The value at 750 nm, where absorption by phytoplankton is negligible, was subtracted from the absorption values across the spectra to account for any scattering, which is assumed to be spectrally flat. The measured absorption coefficients (a, m^{-1}) were then normalized to the cell concentrations to obtain the average cellular absorption cross-sections (σ_a, μm^2). The measured efficiency factors for absorption (Q_a) were determined as $\sigma_a/\overline{G}$. The absorption data presented here are from the spectrophotometer measurements, which were strongly correlated with those from the ac-9 ($r^2 = 0.97$, $n = 208$). On average the ac-9 measurements were 90% of those from the spectrophotometer, but the bias was somewhat wavelength dependent (with ac-9 values lower by as much as 12% at 412 nm or higher by as much as 16% at 650 nm).

For the measurements of chl, triplicate 1-mL samples were collected on GF/F filters and extracted overnight in cold 90% acetone. Samples were analyzed on a 10-AU fluorometer (with optical kit 10-040R, Turner, Sunnyvale, CA, USA) using the non-acidification technique (Welschmeyer 1994). The fluorometer was calibrated with pure chl *a* (Sigma-Aldrich, St. Louis, MO, USA).

For analysis of carbon and nitrogen content, duplicate 25-mL samples were collected on pre-combusted GF/F filters, frozen, and later dried overnight at 60° C. The samples were analyzed on a Perkin-Elmer 2400 CHN analyzer with acetanilide as the standard, and dry pre-combusted filters were analyzed as blanks and subtracted.

Calculations of refractive index. Mie scattering theory, which assumes homogenous and spherical particles, was used to calculate both the real (n) and the imaginary (n′) parts of the refractive index (algorithm from Bohren and Huffman 1983). First, preliminary n′ and then n were calculated using the anomalous diffraction approximation through iterations to closely match the theoretically calculated Q_a (or Q_c) to the experimentally measured Q_a (or Q_c) (Van de Hulst 1957, following equations in Morel and Bricaud 1986, Bricaud and Morel 1986). Then, the final n′ and n were derived from Mie theory using a multidimensional unconstrained nonlinear minimization ("fminsearch" from MATLAB, The MathWorks, Natick, MA, USA) of the absolute value of the difference between measured and theoretical Q_a added to the absolute value of the difference between measured and theoretical Q_c. The measured values used in this estimation of n′ and n are the absorption and attenuation coefficients, cell concentrations, and cell diameter distributions. Calculations were made at eight wavelengths (412, 440, 488, 510, 532, 555, 650, and 676 nm).

RESULTS AND DISCUSSION

Cell growth and division. Micromonas pusilla cell division was phased to the light:dark cycle with most of the division occurring during the first 8 h of darkness (Fig. 1A). The cultures in this experiment were in ultradian growth, with a growth rate over the 24-h experiment of 0.9 d^{-1} (1.3 divisions per day). Approximately one doubling per day took place between dusk and dawn, and the remainder occurred during the light period. Nighttime division is common among eukaryotic phytoplankton in the ocean (Chisholm 1981). A recent study found that cell division in five eukaryotic picoplankton species, including *M. pusilla*, started just before dusk and continued for several hours into the night (Jacquet et al. 2001).

The mean cell volume, $\overline{V}$, increased during the day as the cells were photosynthesizing and then decreased at night upon cell division (Fig. 1A). $\overline{V}$ at the end of the experiment (dawn) was half that at its maximum (dusk), which corresponded to an approximate doubling in cell numbers. This result is expected if we assume that a cell must double in volume before it can divide into two cells and is relevant to the estimation of division rates from cell volume (DuRand and Olson 1998). Mean cell diameter, $\overline{D}$, averaged 1.60 μm with a range of 1.37 to 1.89 μm over the diel cycle. Flow cytometric analysis showed similar patterns in FLS (Fig. 1B) and side light scattering (data not shown). Carbon per cell was also minimum at dawn and maximum at dusk (Fig. 1B). Linear regressions between $\overline{V}$, FLS, and cell carbon all showed strong correlations (between $\overline{V}$ and FLS, $r^2 = 0.91$; between carbon and FLS, $r^2 = 0.92$; between $\overline{V}$ and carbon, $r^2 = 0.93$). The strong relationships between these measurements can be used to interpret diel variations in natural assemblages, for which individual cell carbon content, for example, cannot be measured but FLS of recognizable cell types can.

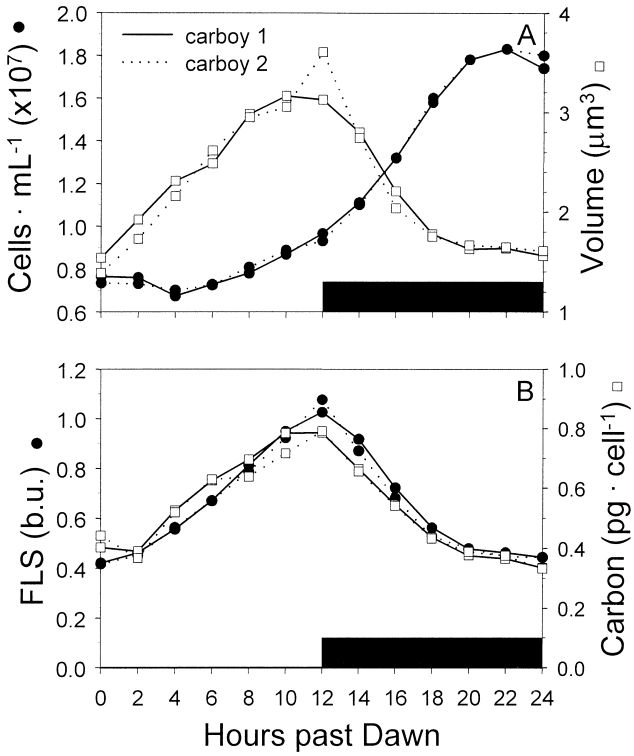

FIG. 1. Time series of (A) cell concentration and cell volume ($\overline{V}$) and (B) flow cytometric forward light scattering (FLS, bead units) and carbon per cell for replicate carboys of *Micromonas pusilla*. The black bar denotes when the lights were off in the incubator (12–24 h past dawn).

Cell constituents and refractive index. For both the real part of the refractive index, n, and the imaginary part of the refractive index, n′, there was no discernible diel pattern that was consistent between the replicate cultures (Fig. 2A). n (650 nm) varied from 1.049 to 1.066 (mean = 1.058, SD = 0.003). n′ (676 nm) varied from 0.0057 to 0.0082 (mean = 0.0066, SD = 0.00052).

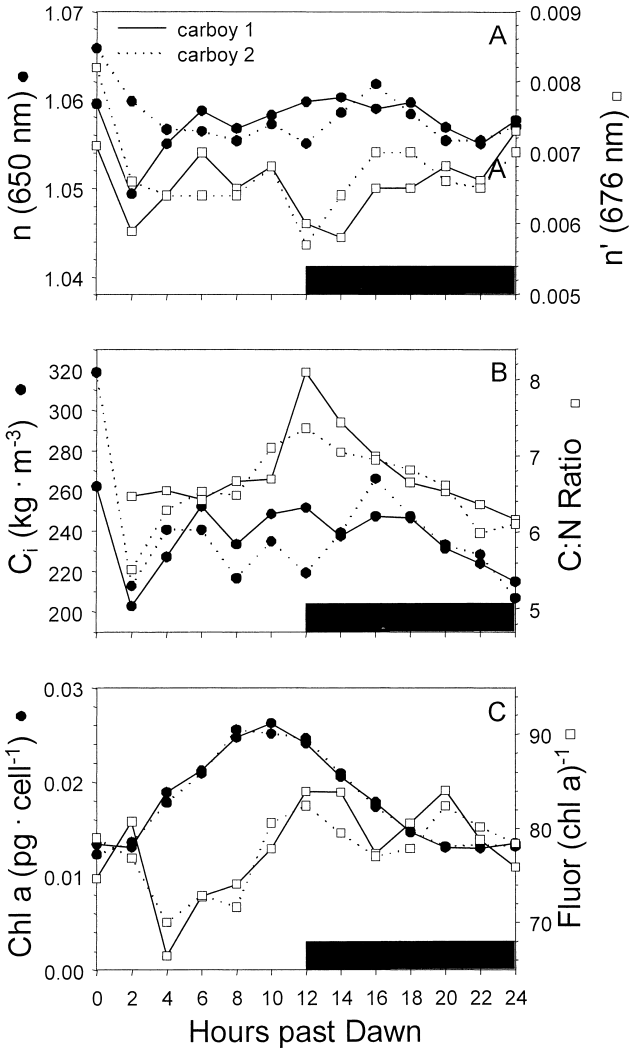

FIG. 2. (A) Time series of the refractive index, n (650 nm), and the imaginary part of the refractive index, n′ (676 nm), for replicate carboys of *Micromonas pusilla*. Values were derived using measurements and Mie scattering theory. (B) Time series of intracellular carbon concentration, C_i (kg•m^{-3}), and C:N ratio and (C) cellular chl concentration (pg•cell^{-1}) and ratio of flow cytometric chl fluorescence to cellular chl a concentration for replicate carboys of *M. pusilla*.

Multiple solutions for n were not found, presumably due to the small size of the cells (see discussion in Stramski and Mobley 1997). Most of the variability in both n′ and n occurred between the first sampling point ("dawn") and the next sampling point (2 h later). The variability in both n and n′ over the 24-h sampling period was small, however, and the calculated values were too noisy to detect a diel pattern. Some of the variability in our estimates of refractive index may be associated with how it was derived. Because n and n′ were calculated from the measured values of absorption and attenuation coefficients, cell size, and cell concentration, any errors in these measurements will be propagated and affect the result of the calculations. Previous studies have shown variability in n with a tendency to increase during the day and decrease at night, though with irregularities, for cultures of *Thalassiosira pseudonana* (Stramski and Reynolds 1993), *Synechococcus* (Stramski et al. 1995), and *Nannochloris* sp. at some growth conditions (DuRand and Olson 1998).

The variation in intracellular carbon concentration, C_i, over time was similar to that of n (Fig. 2B), with no discernible diel pattern. The C:N ratio, however, did not appear to follow trends in n over the diel cycle (Fig. 2B). The daytime increase in C:N ratio, combined with examination of the patterns in particulate organic carbon and particulate organic nitrogen over the day (data not shown), indicates that cells accumulated relatively carbon-rich compounds (carbohydrates) during the day faster than they did nitrogen-rich compounds (proteins). At night, the C:N ratio decreased due to loss of carbon (~20% of total carbon), presumably from respiration, whereas the total nitrogen remained constant. The mean C:N ratio we observed for *M. pusilla* was 6.7, close to the Redfield ratio of 6.6. The common trend found in C_i and n but not in the C:N ratio indicates that changes in the chemical constituents of the cell were less important than the ratio of water to cellular material in determining the refractive index. A similar conclusion was reported by Aas (1996), who calculated n from the composition of phytoplankton cells.

The concentration of chl *a* per cell increased during the day, peaked 2 h before the dark period, and then decreased (Fig. 2C). Flow cytometric chl fluorescence per cell followed a similar diel pattern (data not shown). The ratio of FCM chl fluorescence to cellular chl *a* concentration exhibited a coefficient of variation (CV) of less than 6% over the diel cycle (Fig. 2C), with some indication of a systematic increase in the second half of the light period. The small variations seen here are consistent with low packaging and only minor changes in pigment composition over the course of the day.

Single-cell optical cross-sections and efficiencies. The mean cellular cross-sections for absorption, σ_a, increased during the day and decreased during the night (Fig. 3A). The ratio of FCM chl fluorescence to absorption cross-section (σ_a) showed only small variations, with a CV of 6% over the diel cycle (data not shown). These results suggest that σ_a for these cells can be estimated with reasonable accuracy from measurements of flow cytometric chl fluorescence. This is important for natural samples that include assemblages of mixed species each of which may have very different σ_a values. Different σ_a values cannot be separately assessed by bulk spectrophotometry, but each cell can be independently characterized by flow cytometry.

The mean cellular cross-sections for attenuation, σ_c, increased during the day and decreased during the night (Fig. 3A). The scattering cross-section, σ_b (data not shown), was the major contributor to σ_c (78%–84%). The σ_b obtained from bulk methods includes scattering

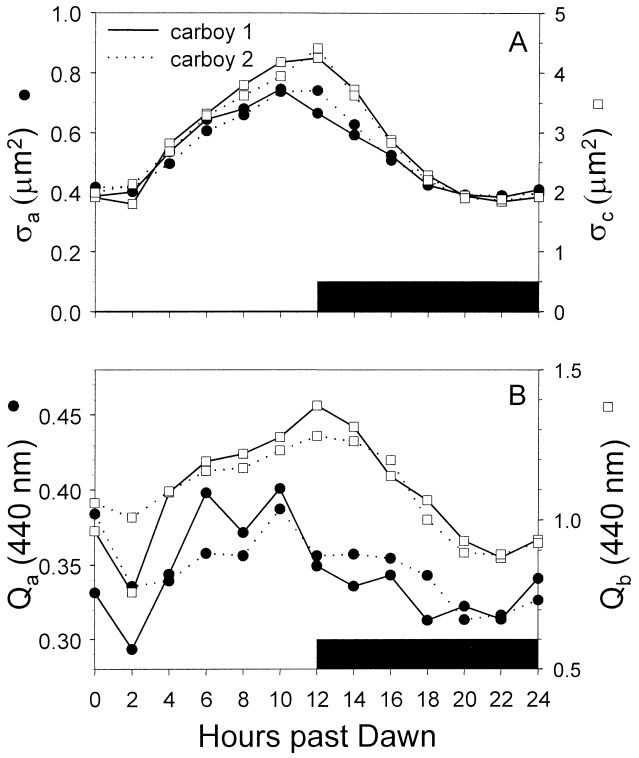

FIG. 3. Time series of (A) optical cross-sections (μm^2 at 488 nm) for absorption (σ_a) and attenuation (σ_c) for replicate carboys of *Micromonas pusilla*. Note that the *y*-axes are scaled differently. (B) Time series of efficiency factors for absorption, Q_a, and scattering, Q_b, both at 440 nm for replicate carboys of *M. pusilla*.

from all angles; nonetheless it was strongly correlated with FLS from the flow cytometer ($r^2 = 0.94$). It is important for interpreting measurements on natural samples that FLS values for the angles measured by the flow cytometer strongly contribute to total scattering.

The efficiency factor for absorption, Q_a (440 nm), tended to increase during the day, reached a peak 2 h before dusk, and then decreased, though the pattern was not striking (Fig. 3B). As with n′, the diel pattern in Q_a was not dramatic, because the variations over the course of the diel cycle were small and the data were noisy. The Q_a values were low, which is consistent with little packaging. The efficiency factor for scattering, Q_b (440 nm), clearly increased during the day and decreased during the night (Fig. 3B). These variations were driven primarily by changes in cell size (Fig. 1A). The observed variations in n (which were similar at 440 nm to those at 650 nm in Fig. 2A) were not large enough to noticeably influence the diel pattern in Q_b.

Bulk optical properties. The chl-specific absorption coefficient (a^*_{chl}) did not exhibit a diel pattern (Fig. 4A) even at 440 nm, the wavelength at which the most variability is expected due to potential changes in the package effect and in pigment composition. This indicates that the package effect is negligible for *M. pusilla*, which is consistent with the findings for other picoplankton-sized cells (Stramski et al. 1995). The mean a^*_{chl} at 676 nm was 0.0201 $m^2 \cdot (mg\ chl)^{-1}$ (range over time was 0.0180 to 0.0229), which is extremely close to the value for pure chl a dissolved in acetone (0.0207 at 663 nm; Morel and Bricaud 1986). This is also consistent with virtually no package effect in these cells.

The chl-specific scattering coefficient (b^*_{chl}), though relatively constant during most of the light period, increased shortly before dusk, peaked near dusk, and then declined during the dark period (Fig. 4A). The peak near dusk was likely due to the slight time lag between the peak in bulk chl concentration (10 h) and the peak in bulk carbon concentration (12 h); this lag suggests that the cells stopped synthesizing chl before they stopped producing other cell material. The diel variations we observed in b^*_{chl} (21% increase from dawn

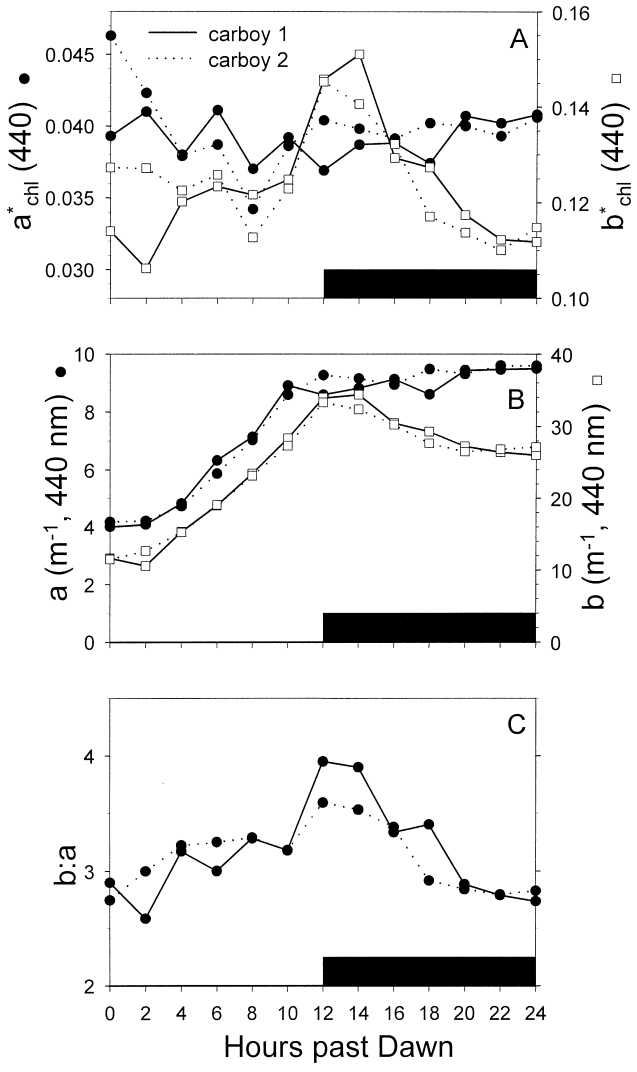

FIG. 4. Time series of (A) chl-specific absorption (a^*_{chl}, $m^2 \cdot (mg\ chl)^{-1}$) and chl-specific scattering (b^*_{chl}, $m^2 \cdot (mg\ chl)^{-1}$); (B) absorption coefficient, a (m^{-1}), and scattering coefficient, b (m^{-1}); and (C) scattering-to-absorption ratio, *b:a*, all at 440 nm for replicate carboys of *Micromonas pusilla*.

to dusk) were small compared with the variations among species, which have been found to be 8- to 10-fold (Bricaud et al. 1983, Morel 1987). This implies that chl-based models of scattering (such as Morel 1987) should be relatively insensitive to the time of day the measurements were taken, even for phytoplankton that exhibit phased division patterns.

The bulk absorption coefficient a (440 nm) (Fig. 4B) increased during the day and then was relatively constant during the night. The daytime increase was primarily caused by the increase in chl per cell (Fig. 2C) and associated increase in σ_a (Fig. 3A) and not to cell concentration, which was relatively constant (Fig. 1A). In contrast, the constant values of a at night reflect a balance between increasing cell concentration (Fig. 1A) and decreasing σ_a (Fig. 3A). These results are also consistent with a negligible package effect because a did not increase during the night when the cells were getting smaller. As a result, the pattern in a reflects that of bulk chl in the culture, which also increased during the day and was constant at night (data not shown).

The bulk scattering coefficient b (440 nm) exhibited a daytime increase similar to a (440 nm), but in contrast to a, b decreased during the night (Fig. 4B). The daytime increase was primarily caused by the increase in diameter and associated increase in σ_b per cell and not by changes in n or cell concentration, which were both relatively constant (Figs. 1A and 2A). The nighttime decrease in b is predicted theoretically for cells of this size undergoing division. Even though the redistribution of cell material from one cell (diameter = 1.8 μm pre-division) to two smaller cells (assuming conservation of volume) results in a 26% increase in the sum of the geometric cross-sections, theory predicts a 10% decrease in b (440 nm) (using the anomalous diffraction approximation with n′ and n set to the average values, 0.0095 and 1.057, respectively). The observed scattering coefficients for these *M. pusilla* cultures showed a decrease of approximately 20% during the nighttime division period. There are several possible explanations for the larger decrease than that predicted by theory. It could be due, in part, to losses of cell carbon through respiration; bulk carbon concentration in the culture decreased by approximately 20% during the night hours. In addition, the effects of intracellular heterogeneity and changes in cell shape upon division that cannot be accounted for by Mie theory could also contribute. Changes in the refractive index may also be a factor; however, the changes observed were not consistent (n increased in one culture and decreased slightly in the replicate), suggesting that this is not a significant factor determining the observed variability in b (which decreased in both replicate cultures during the night).

The ratio of scattering to absorption, b:a, at 440 nm tended to increase during the day and decrease during the night (Fig. 4C). The average value for b:a for *M. pusilla* was 3.14 (CV = 11% over diel cycle), which is in the range observed for other types of phytoplankton (Stramski and Mobley 1997). In the ocean b:a may be affected by the planktonic community composition, with higher values expected for a community with a significant heterotrophic bacterial contribution, for example. This example for pure phytoplankton and the variations observed over the diel cycle should be useful for interpreting absorption and scattering coefficients from *in situ* instruments such as ac-9 meters (e.g. Sosik et al. 2001).

Spectral variability. The spectral shape of a did not vary with time of day, but the spectral shape of b did (Fig. 5A). As an indicator of the shape of the b spectrum, a spectral slope (γ) was estimated for each observation based on least-squares regression to a power function: $b(\gamma) = \alpha \cdot \lambda^{-\gamma}$, where α and γ are fit parameters. Values of γ varied systematically with cell size, with the greatest values occurring when the cells were smallest (Fig. 5B). *In situ* instruments capable of quantifying the spectral shape of both a and b are now in common use, and this kind of information about potential sources and amplitudes of variation will be critical for adequate interpretation of observations from natural waters.

Both parts of the refractive index, n and n′, also exhibited spectral variability, although with no discernible change over the course of the day (Fig. 6). The observed spectral shape of n is similar to that previ-

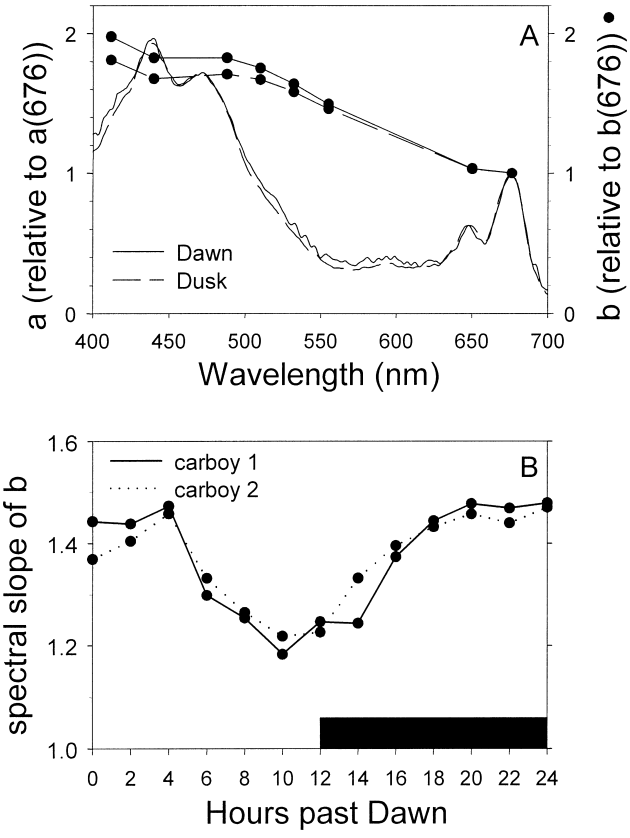

FIG. 5. A) Spectral absorption (a) and scattering (b) coefficient normalized to 676 nm for two time points, dawn and dusk, for *Micromonas pusilla* carboy 1. (B) Time series of the spectral slope of b, γ, for the replicate carboys.

ously observed for another picophytoplankton, *Synechococcus* ("CYA" in Stramski and Mobley 1997). Both spectra exhibited a maximum near 490 nm and also increased in the red part of the spectrum. The spectral shape of n′, the part of the refractive index attributable to absorption, was similar to that of *a* (Fig. 5A).

Size and refractive index effects on attenuation. To evaluate the relative effects of variations in cell size and variations in refractive index on the attenuation cross-section (σ_c), a sensitivity analysis was performed. We used Mie scattering theory to calculate Q_c and σ_c (at 650 nm) from estimates of n, n′, and measured $\overline{D}$. A series of calculations were made with either n′ and n or $\overline{D}$ held constant at the observed mean values, whereas the other input(s) were allowed to vary with the observed diel pattern. The theoretical σ_c values derived with constant n′ and n and with varying $\overline{D}$ closely matched the measured σ_c values, whereas those calculated with constant $\overline{D}$ and varying n′ and n were nearly constant over the diel cycle (Fig. 7). These calculations emphasize that variation in cell size for *M. pusilla* is the primary factor determining the diel variability in σ_c. This is similar to the results found in a diel study of *Nannochloris* sp. (DuRand and Olson 1998), where variations in cell size were a more important source of change in attenuation than variations in refractive index. For the diatom *Thalassiosira pseudonana* (Stramski and Reynolds 1993) and for the prokaryotic *Synechococcus* (Stramski et al. 1995), however, variations in n were found to be more important or equal in importance to variations in cell size. This difference may arise because *Synechococcus* cells do not exhibit highly synchronized cell division (Binder and Chisholm 1995) and because *T. pseudonana* is a diatom and thus has constraints on its size set by its silica frustule and, additionally, may not be expected to have tightly synchronized cell division (Chisholm et al. 1980).

Interspecific variability in carbon-specific attenuation. The carbon-specific attenuation (c_c^*) at 650 nm (Fig. 8) increased during the day and decreased at night for *M. pusilla.* The variation over the diel cycle was approximately 30% of the value at dawn, which is comparable with the variation of 25%–30% between dawn and dusk previously reported for *T. pseudonana* (Stramski and Reynolds 1993), *Synechococcus* sp. (Stramski et al. 1995), and *Nannochloris* sp. (DuRand and Olson 1998). The mean value of c_c^* we observed for *M. pusilla* was 2.9 $m^2 \cdot (g\ C)^{-1}$, within the range of 2.5 to 3.8 $m^2 \cdot (g\ C)^{-1}$ reported for the other species. Among these four species of phytoplankton that have been investigated in laboratory studies over the diel cycle, as well as *Synechocystis* that has been studied over a range of different light levels (Stramski and Morel 1990), c_c^* varies systematically with cell size (Fig. 9). The range of values for c_c^* among species is greater than the variability over the diel cycle for a single species. Nonetheless, the intraspecific variability (for *M. pusilla* and *Nannochloris* sp., at least) did show the same pattern: in-

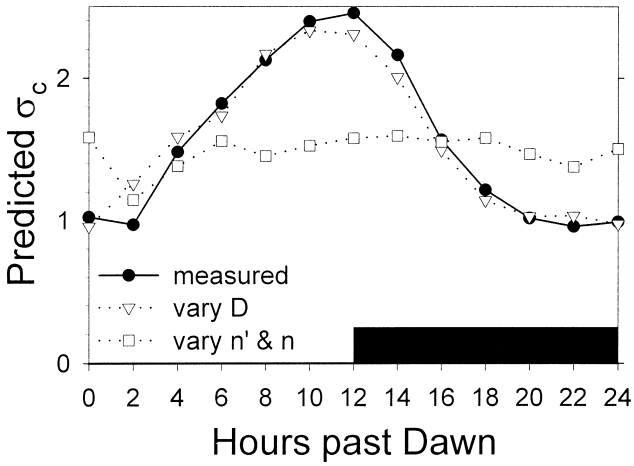

FIG. 7. Results of sensitivity analysis for effects of varying diameter ($\overline{D}$, with n and n′ constant) or varying refractive index (n′ and n, with $\overline{D}$ constant) on the predicted attenuation cross-section, σ_c. For comparison, the measured σ_c for *Micromonas pusilla* carboy 1 are also shown (results for the replicate carboy were similar).

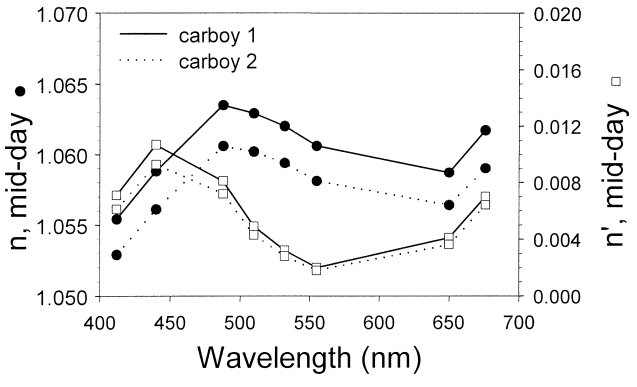

FIG. 6. Spectra of the real part of the refractive index (n) and the imaginary part of the refractive index (n′) both at midday (6 h after dawn) for replicate carboys of *Micromonas pusilla.*

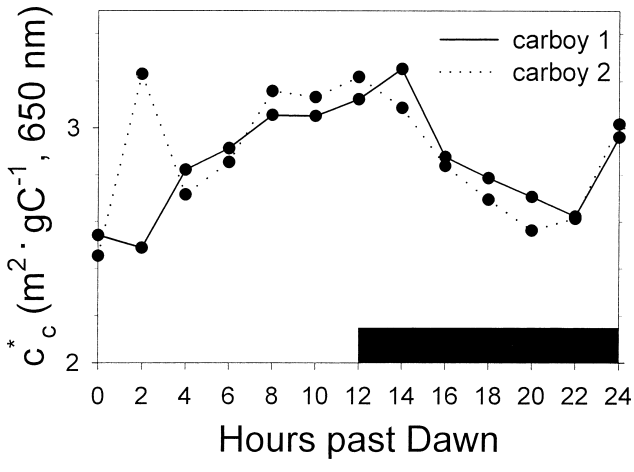

FIG. 8. Time series of carbon-specific attenuation coefficient (c_c^*, $m^2 \cdot (g\ C)^{-1}$ at 650 nm) for replicate carboys of *Micromonas pusilla.*

creasing c_c^* with increasing size over the diel cycle (data not shown). Several investigators used a single value of c_c^* to relate *in situ* measurements of beam attenuation to carbon concentration for estimates of production from diel studies (Siegel et al. 1989, Cullen et al. 1992, Walsh et al. 1995). These results indicate that it is important to consider not only diel variations in c_c^* but also variability with community structure (DuRand and Olson 1996) because c_c^* appears to vary systematically with phytoplankton cell size.

Relating FLS to cell size. An important outgrowth of laboratory-based experiments on phytoplankton optical properties is their application to studies in natural waters with mixed assemblages of cell types. This is especially relevant for flow cytometric studies where several different groups of phytoplankton can be distinguished in natural samples. In a number of studies, investigators have used cell concentrations from flow cytometry of different phytoplankton groups to calculate their contribution to microbial carbon using an empirical factor or calibration to convert from assumed or measured cell size to carbon (Li et al. 1992, Campbell et al. 1994, 1997). Some recent studies of natural assemblages have been based on a similar approach, but in these cases cell volume was determined from FLS measurements and an empirical relationship for phytoplankton cultures and then volume was converted to carbon content via a second empirical relationship (Gin et al. 1999, DuRand et al. 2001, Shalapyonok et al. 2001). In addition, it has been suggested that diel variations in phytoplankton light scattering in natural samples can be used to estimate phytoplankton growth rates (DuRand 1995, Binder et al. 1996, DuRand and Olson 1998, Vaulot and Marie 1999), with some caveats, such as potential complication by changes in refractive index. This application is supported by our finding that a large-scale calibration between FLS and cell size based on a wide range of different sized phytoplankton (equivalent spherical diameter from 0.87 to 39 μm) also applies over the smaller size range (approximately doubling) that occurs in a single species over the diel cycle (Fig. 10). The data presented here do not reflect a comprehensive study of different species and growth conditions, and it is possible that factors such as variations in the pigments that absorb at 488 nm (the wavelength of the FCM laser), differences in cell shape and internal structures, and changes in scattering efficiency with cell size may add additional unexplained variance to the relationship shown in Figure 10. Even considering these limitations, using FLS to estimate cell volume has advantages over assuming a mean size for all cells in a population or assemblage because it provides a means to examine diel and other high frequency variations.

Relating optical properties to carbon and chl. For many ecological questions, determining cell volume is an intermediate step toward estimating biomass (e.g. carbon

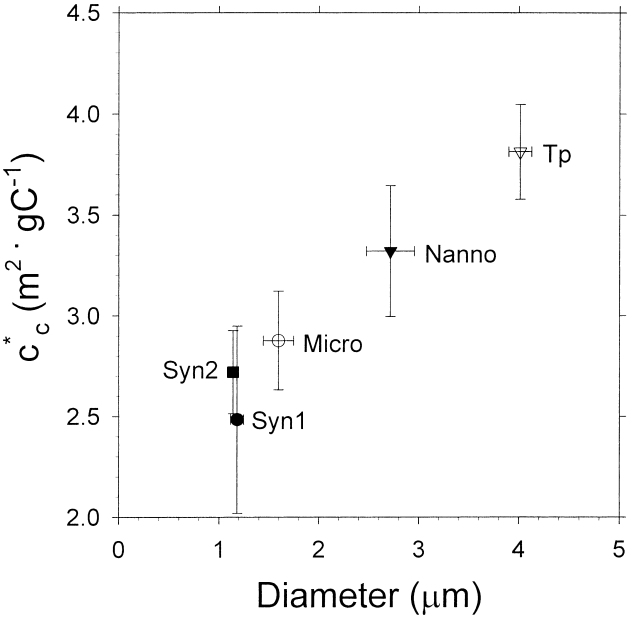

FIG. 9. Relationship between the carbon-specific beam attenuation (c_c^*, $m^2 \cdot (g\ C)^{-1}$) and diameter for five different phytoplankton: *Synechococcus* ("Syn1," Stramski et al. 1995), *Synechocystis* ("Syn2," Stramski and Morel 1990), *Micromonas pusilla* ("Micro," this study), *Nannochloris* sp. ("Nanno," DuRand and Olson 1998), and *Thalassiosira pseudonana* ("Tp," Stramski and Reynolds 1993). For each data point the mean ± SD over the diel cycle is shown, except for Syn2 for which the mean ± SD for seven different irradiances is shown. The c_c^* is at 650 nm for all except Syn2 at 660 nm.

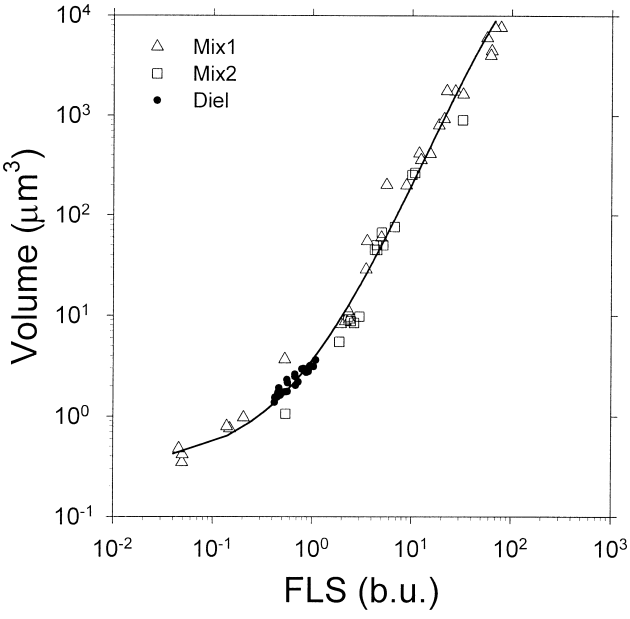

FIG. 10. Relationship between cell volume (μm^3) and flow cytometric forward light scattering (FLS, bead units). "Mix1" indicates measurements on different phytoplankton species at one time of day (25 batch phytoplankton cultures consisting of 10 dinoflagellates, 5 prymnesiophytes, 4 *Synechococcus* strains, 3 prasinophytes, 2 chlorophytes, and 1 diatom; $n = 33$ because some cultures were measured on more than one occasion). "Mix2" designates measurements on a number of different phytoplankton species (Green 2002, Green et al. in press). "Diel" indicates data from the *M. pusilla* diel sampling experiment. The line shows a fourth-order polynomial fit, $r^2 = 0.98$, for both "Mix" data sets.

or chl). Because relationships between cell volume and light scattering can be complicated, more direct approaches to estimating cell biomass from optical properties have been examined. Significant positive relationships between C_i and n and between intracellular chl concentration and n′ have been established from laboratory experiments on phytoplankton cultures (Stramski and Reynolds 1993, Stramski et al. 1995, DuRand and Olson 1998, Stramski 1999, Stramski et al. 2002). The diel variations we observed in *M. pusilla* are consistent with general relationships that describe results from a variety of phytoplankton cultures (Fig. 11). Stramski (1999) suggested that individual particle analysis of natural samples could yield information about the refractive index of different types of microorganisms that could then be converted to C_i and intracellular chl concentration that, together with data on cell size, could be used to estimate contributions of different particle types to carbon and chl concentration in the ocean. This approach is based on theoretical considerations and empirical data but does not require the potentially problematic conversion from cell volume to carbon content. The most difficult component of this approach is determining refractive index from individual particle optical measurements in natural samples; although some limited estimates of real refractive index have been made (Ackleson and Robins 1990), it is not a routine measurement with currently available instrumentation. (Green 2002, Green et al. in press) investigated this extensively with flow cytometry and concluded that large real refractive index differences, such as between phytoplankton and mineral particles, can be resolved. It is clear, however, that differences among phytoplankton are difficult to quantify accurately. Estimates of refractive index with this approach are limited in accuracy by required assumptions about particle homogeneity and shape.

We propose instead that cellular carbon content be directly estimated from flow cytometric measurements of FLS. Cellular carbon content and FLS are well correlated (Fig. 12, $r^2 = 0.98$) over a large range of phytoplankton species and cell sizes; though it is not a comprehensive study, this data set does include variability over the diel cycle and over different irradiance levels and growth conditions. The exact details of the relationship we present are specific to our flow cytometer and its optical configuration, but a similar calibration could be obtained with relative ease for other instruments. Using our laboratory-based calibration to convert FLS to cellular carbon content will allow us to estimate the contribution of different plankton groups to total carbon content in the oceans with simple flow cytometric counts and measurements of FLS. This "FLS-carbon method" should be more reliable than empirical conversion of cell volume to carbon content (reviewed by Stramski 1999). Much of the variability in cell volume to carbon relationships is associated with differences in cell constituent concentrations (i.e. carbon and water content) that also affect refractive index. Because FLS is affected by both cell volume and refractive index, the relationship between FLS and cellular carbon is subject to less variability than the relationships between FLS and cell volume or between cell volume and carbon content. Even though this is not apparent in our data for *M.*

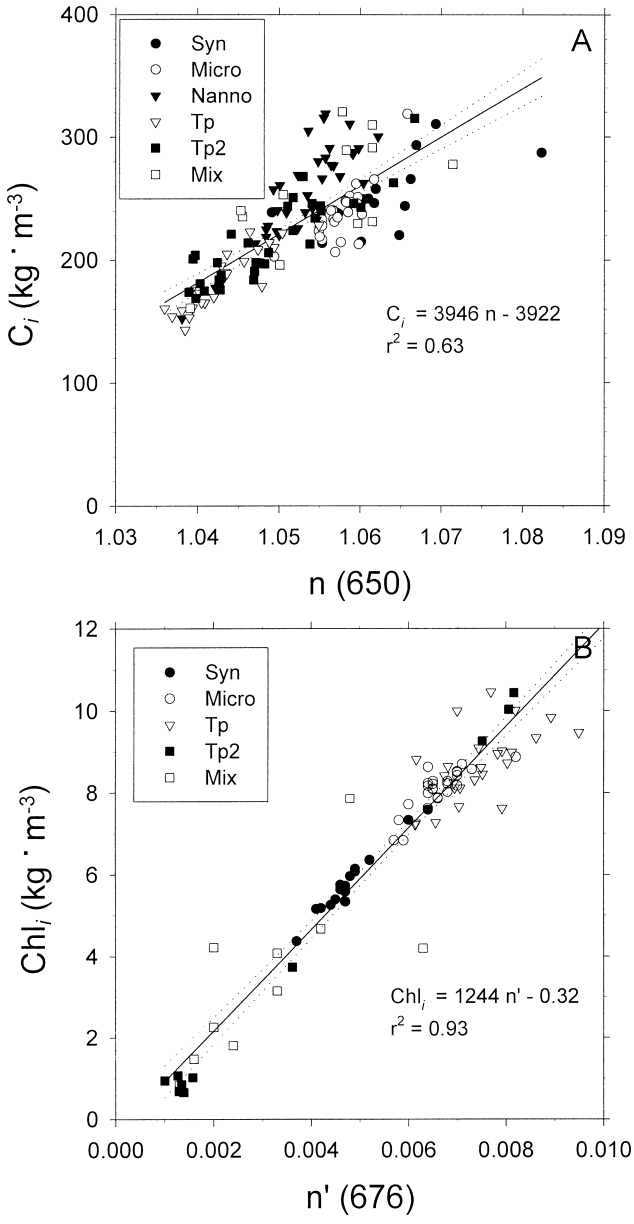

FIG. 11. (A) Relationship between real refractive index, n(650), and intracellular carbon concentration, C_i, for *Synechococcus* ("Syn," Stramski et al. 1995), *Micromonas pusilla* ("Micro," this study), *Nannochloris* sp. ("Nanno," DuRand and Olson 1998), *Thalassiosira pseudonana* ("Tp," Stramski and Reynolds 1993, Stramski 1999 and "Tp2," Stramski et al. 2002), and a number of different phytoplankton species ("Mix," Green et al. in press, Green 2002). Data for n are at 660 nm for Syn, Nanno, Tp, and Tp2. Linear regression and 95% confidence intervals are plotted. (B) Relationship between imaginary refractive index, n′(676), and intracellular chl concentration, Chl_i, for the same experiments as in A, excluding Nanno. Data for n′ are at 675 nm for Syn and Tp and at 674 nm for Tp2. Linear regression and 95% confidence intervals are plotted.

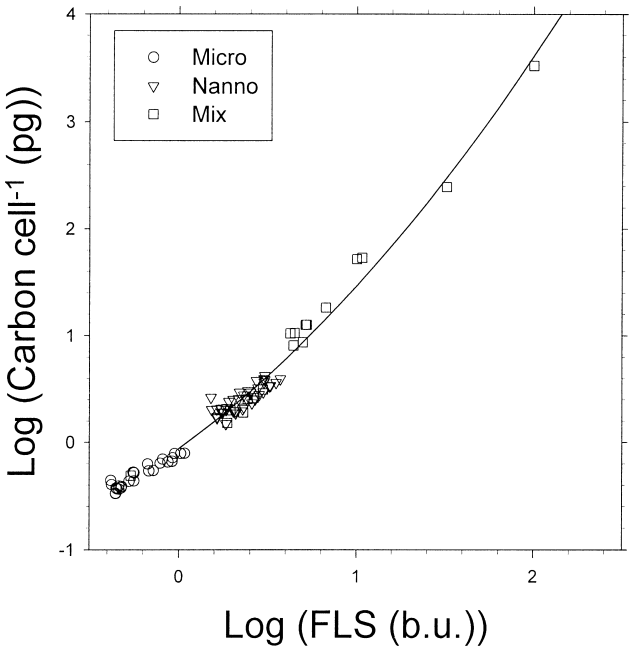

FIG. 12. Relationship between FLS (b.u.) and cellular carbon content (pg·cell^{-1}) for *Micromonas pusilla* ("Micro," this study), *Nannochloris* sp. ("Nanno," DuRand and Olson 1998), and a number of different phytoplankton species ("Mix," Green 2002, Green et al. in press). A second-order polynomial fit to the log data is shown ($r^2 = 0.98$).

pusilla (because variations in n were small), it was evident in a study of *Nannochloris* grown under different conditions (DuRand 1995, DuRand and Olson 1998). In addition, the FLS-carbon method is not susceptible to errors associated with deriving n and cell size using Mie scattering theory and the inherent assumptions of sphericity and homogeneity. Even though scattering theory indicates FLS is not a monotonic function of cell size and refractive index, we have found a strong correlation between cellular carbon content and FLS. Further work is required to determine how sensitive this relationship is to other factors that would be expected to add variability, such as inclusion of cells that contain coccoliths or gas vacuoles or that have highly elongated shapes. Despite these caveats we suggest that routine FLS measurements, coupled with an empirical relationship between FLS and cellular carbon such as that presented here, could provide simple estimates of the carbon content of different planktonic microorganisms and thus yield important information on the partitioning and size distribution of carbon in the oceans. In addition, because variations over the diel cycle in this relationship fall on the same line as the general relationship, diel changes in FLS could be converted to diel changes in carbon content, thus allowing carbon productivity to be determined for groups of phytoplankton similar to *M. pusilla*.

Conclusions. Even though they are ubiquitous in the oceans, eukaryotic picophytoplankton have not been subject to detailed optical analysis until the present study of *M. pusilla*. Because phasing to the light:dark cycle is a widespread occurrence, we investigated diel variations in physical, chemical, and optical properties and found that *M. pusilla* cells increased in cell size, carbon content, single-cell scattering, attenuation, and absorption during the light period; all these properties then decreased with cell division during the dark period. Neither the real nor the imaginary refractive indices showed any significant trend over the light:dark cycle.

The relationships between optical properties and physical or chemical cell characteristics observed for *M. pusilla* over the diel cycle were similar to trends observed across a range of species. With regard to single-cell light scattering, this is consistent with our finding that changes in refractive index of *M. pusilla* over the diel cycle were small (i.e. that light scattering was affected by cell size primarily). More generally, these results suggest that empirical approaches for estimating cell properties from light scattering measurements are applicable to a wide variety of species. In particular, we propose that the relationship observed between flow cytometric FLS and cellular carbon will allow estimation of the carbon content of different phytoplankton groups in natural assemblages. For cells similar to *M. pusilla*, the relationship can also be used to resolve diel variations related to cell growth and division.

In many natural communities, eukaryotic phytoplankton are numerically dominated by cells similar to *M. pusilla*. The ability to estimate their cell size and carbon content, population growth rates and primary productivity, and contributions to bulk optical properties such as beam attenuation will expand our understanding of the role these cells play in planktonic ecosystems.

We are grateful to Anne Canaday and Alexi Shalapyonok for assistance in the laboratory. We also thank Rick Reynolds and Dariusz Stramski for providing their data. Supported by NASA grants NAGW-5217, NAG5-7538, and NAG5-8868 (to H. M. S.) and ONR grant N000149510333 (to H. M. S. and R. J. O.). This is WHOI contribution 10608.

Aas, E. 1996. Refractive index of phytoplankton derived from its metabolite composition. *J. Plankton Res.* 18:2223–49.

Ackleson, S. G. and Robins, D. B. 1990. Flow cytometric determinations of North Sea phytoplankton optical properties. *Neth. J. Sea Res.* 25:11–8.

Ackleson, S. G., Cullen, J. J., Brown, J. & Lesser, M. 1993. Irradiance-induced variability in light scatter from marine phytoplankton in culture. *J. Plankton Res.* 15:737–59.

Binder, B. J. & Chisholm, S. W. 1995. Cell cycle regulation in marine *Synechococcus* sp. strains. *Appl. Environ. Microbiol.* 61:708–17.

Binder, B. J., Chisholm, S. W., Olson, R. J., Frankel, S. L. & Worden, A. Z. 1996. Dynamics of picophytoplankton, ultraphytoplankton, and bacteria in the central equatorial Pacific. *Deep-Sea Res. II* 43:907–31.

Binder, B. J. & DuRand, M. D. 2002. Diel cycles in surface waters of the equatorial Pacific. *Deep-Sea Res. II* 49:2601–17.

Bohren, C. F. & Huffman, D. R. 1983. *Absorption and Scattering of Light by Small Particles.* John Wiley & Sons, New York, 530 pp.

Bricaud, A., Morel, A. & Prieur, L. 1983. Optical efficiency factors of some phytoplankters. *Limnol. Oceanogr.* 28:816–32.

Bricaud, A. & Morel, A. 1986. Light attenuation and scattering by phytoplanktonic cells: a theoretical modeling. *Appl. Opt.* 25: 571–80.

Campbell, L. Nolla, H. A. & Vaulot, D. 1994. The importance of *Prochlorococcus* to community structure in the central North Pacific Ocean. *Limnol. Oceanogr.* 39:954–61.

Campbell, L., Liu, H., Nolla, H. A. & Vaulot, D. 1997. Annual variability of phytoplankton and bacteria in the subtropical North Pacific Ocean at Station ALOHA during the 1991–1994 ENSO event. *Deep-Sea Res. I* 44:167–92.

Chisholm, S. W. 1981. Temporal patterns of cell division in unicellular algae. *Can. Bull. Fish. Aquat. Sci.* 210:150–81.

Chisholm, S. W., Morel, F. M. M. & Slocum, W. S. 1980. The phasing and distribution of cell division cycles in marine diatoms. *Environ. Sci. Res.* 19:281–300.

Chung, S. P., Gardner, W. D., Landry, M. R., Richardson, M. J. & Walsh, I. D. 1998. Beam attenuation by microorganisms and detrital particles in the equatorial Pacific. *J. Geophys. Res.* 103:12669–81.

Cullen, J. J., Lewis, M. R., Davis, C. O. & Barber, R. T. 1992. Photosynthetic characteristics and estimated growth rates indicate grazing is the proximate control of primary production in the equatorial Pacific. *J. Geophys. Res.* 97:639–54.

Diez, B., Pedros-Alio, C. & Massana, R. 2001. Study of genetic diversity of eukaryotic picoplankton in different oceanic regions by small-subunit rRNA gene cloning and sequencing. *Appl. Environ. Microbiol.* 67:2932–41.

DuRand, M. D. 1995. *Phytoplankton Growth and Diel Variations in Beam Attenuation through Individual Cell Analysis.* Ph.D. thesis. Massachusetts Institute of Technology/Woods Hole Oceanographic Institution, Woods Hole, MA, 263 pp.

DuRand, M. D. & Olson, R. J. 1996. Contributions of phytoplankton light scattering and cell concentration changes to diel variations in beam attenuation in the equatorial Pacific from flow cytometric measurements of pico-, ultra-, and nanoplankton. *Deep-Sea Res. II* 43:891–906.

DuRand, M. D. & Olson, R. J. 1998. Diel patterns in optical properties of the chlorophyte *Nannochloris* sp.: relating individual-cell to bulk measurements. *Limnol. Oceanogr.* 43:1107–18.

DuRand, M. D., Olson, R. J. & Chisholm, S. W. 2001. Phytoplankton population dynamics at the Bermuda Atlantic Time-series station in the Sargasso Sea. *Deep-Sea Res. II* 48:1983–2003.

Gardner, W. D., Walsh, I. D. & Richardson, M. J. 1993. Biophysical forcing of particle production and distribution during a spring bloom in the North Atlantic. *Deep-Sea Res. II* 40:171–95.

Gardner, W. D., Chung, S. P., Richardson, M. J. & Walsh, I. D. 1995. The oceanic mixed-layer pump. *Deep-Sea Res. II* 42:757–75.

Gin, K. Y. H., Chisholm, S. W. & Olson, R. J. 1999. Seasonal and depth variation in microbial size spectra at the Bermuda Atlantic time series station. *Deep-Sea Res. I* 46:1221–45.

Green, R. E. 2002. *Scale Closure in Upper Ocean Optical Properties: From Single Particles to Ocean Color.* Ph.D. thesis. Massachusetts Institute of Technology/Woods Hole Oceanographic Institution, Woods Hole, MA, 168 pp.

Green, R. E., Sosik, H. M., Olson, R. J. & DuRand, M. D. Flow cytometric determination of size and complex refractive index for marine particles: Comparison with independent bulk estimates. *Appl. Opt.* (in press).

Guillard, R. R. L. 1975. Culture of phytoplankton for feeding marine invertebrates. *In* Smith, W. & Chaney, M. [Eds.] *Culture of Marine Invertebrate Animals.* Plenum, New York, pp. 29–60.

Hamilton, M., Granata, T. C., Dickey, T. D., Wiggert, J. D., Siegel, D. A., Marra, J. & Langdon, C. 1990. Diel variations of bio-optical properties in the Sargasso Sea. *SPIE: Ocean Optics X* 1302:214–24.

Jacquet, S., Partensky, F., Lennon, J. & Vaulot, D. 2001. Diel patterns of growth and division in marine picoplankton in culture. *J. Phycol.* 37:357–69.

Jerlov, N. G. 1976. *Marine Optics.* Elsevier, Amsterdam, 231 pp.

Li, W. K. W., Dickie, P. M., Irwin, B. D. & Wood, A. M. 1992. Biomass of bacteria, cyanobacteria, prochlorophytes and photosynthetic eukaryotes in the Sargasso Sea. *Deep-Sea Res.* 39:501–19.

Morel, A. 1987. Chlorophyll-specific scattering coefficient of phytoplankton. A simplified theoretical approach. *Deep-Sea Res.* 34: 1093–105.

Morel, A. & Bricaud, A. 1986. Inherent optical properties of algal cells including picoplankton: theoretical and experimental results. *Can. Bull. Fish. Aquat. Sci.* 214:521–59.

Not, F., Simon, N., Biegala, I. C. & Vaulot, D. 2002. Application of fluorescent *in situ* hybridization coupled with tyramide signal amplification (FISH-TSA) to assess eukaryotic picoplankton composition. *Aquat. Microb. Ecol.* 28:157–66.

Olson, R. J., Chisholm, S. W., Zettler, E. R. & Armbrust, E. V. 1990. Pigments, size, and distribution of *Synechococcus* in the North Atlantic and Pacific Oceans. *Limnol. Oceanogr.* 35:45–58.

Pegau, W. S., Gray, D. & Zaneveld, J. R. V. 1997. Absorption and attenuation of visible and near-infrared light in water: dependence on temperature and salinity. *Appl. Opt.* 36:6035–46.

Reynolds, R. A., Stramski, D. & Kiefer, D. A. 1997. The effect of nitrogen limitation on the absorption and scattering properties of the marine diatom *Thalassiosira pseudonana. Limnol. Oceanogr.* 42:881–92.

Shalapyonok, A., Olson, R. J. & Shalapyonok, L. S. 2001. Arabian Sea phytoplankton during Southwest and Northeast Monsoons 1995: composition, size structure and biomass from individual cell properties measured by flow cytometry. *Deep-Sea Res. II* 48: 1231–61.

Siegel, D. A., Dickey, T. D., Washburn, L., Hamilton, M. K. & Mitchell, B. G. 1989. Optical determination of particulate abundance and production variations in the oligotrophic ocean. *Deep-Sea Res.* 36:211–22.

Sosik, H. M., Green, R. E., Pegau, W. S. & Roesler, C. S. 2001. Temporal and vertical variability in optical properties of New England shelf waters during late summer and spring. *J. Geophys. Res.* 106:9455–72.

Stramska, M. & Dickey, T. D. 1992. Variability of bio-optical properties of the upper ocean associated with diel cycles in phytoplankton populations. *J. Geophys. Res.* 97:17873–87.

Stramski, D. 1999. Refractive index of planktonic cells as a measure of cellular carbon and chlorophyll *a* content. *Deep-Sea Res. I* 46: 335–51.

Stramski, D. & Morel, A. 1990. Optical properties of photosynthetic picoplankton in different physiological states as affected by growth irradiance. *Deep-Sea Res.* 37:245–66.

Stramski, D. & Reynolds, R. A. 1993. Diel variations in the optical properties of a marine diatom. *Limnol. Oceanogr.* 38:1347–64.

Stramski, D., Shalapyonok, A. & Reynolds, R. A. 1995. Optical characterization of the oceanic unicellular cyanobacterium *Synechococcus* grown under a day-night cycle in natural irradiance. *J. Geophys. Res.* 100:13295–307.

Stramski, D. & Mobley, C. D. 1997. Effects of microbial particles on ocean optics: a database of single-particle optical properties. *Limnol. Oceanogr.* 42:538–49.

Stramski, D., Sciandra, A. & Claustre, H. 2002. Effects of temperature, nitrogen, and light limitation on the optical properties of the marine diatom *Thalassiosira pseudonana. Limnol. Oceanogr.* 37:392–403.

Van de Hulst, H. C. 1957. *Light Scattering by Small Particles.* John Wiley & Sons, New York, 470 pp.

Vaulot, D. & Marie, D. 1999. Diel variability of photosynthetic picoplankton in the equatorial Pacific. *J. Geophys. Res.* 104:3297–310.

Walsh, I. D., Chung, S. P., Richardson, M. J. & Gardner, W. D. 1995. The diel cycle in the integrated particle load in the equatorial Pacific: A comparison with primary production. *Deep-Sea Res. II* 42:465–77.

Welschmeyer, N. A. 1994. Fluorometric analysis of chlorophyll a in the presence of chlorophyll b and pheopigments. *Limnol. Oceanogr.* 39:1985–92.

Zubkov, M., Sleigh, M., Tarran, G., Burkill, P. & Leakey, R. 1998. Picoplanktonic community structure on an Atlantic transect from 50 degree N to 50 degree S. *Deep-Sea Res. I* 45:1339–55.